

## Bulk Excitonic Effects in Surface Optical Spectra

P. H. Hahn, W. G. Schmidt, and F. Bechstedt

*Institut für Festkörpertheorie und Theoretische Optik, Friedrich-Schiller-Universität, Max-Wien-Platz 1, 07743 Jena, Germany*  
(Received 11 July 2001; published 17 December 2001)

We calculate the surface optical properties of the passivated Si(110) surface using a real-space multi-grid technique and *ab initio* pseudopotentials. Rather than from the usual eigenvalue representation, the macroscopic polarizability is obtained from the solution of an initial-value problem, which allows inclusion of excitonic and local-field effects in addition to the electronic self-energy in the surface calculations. It is shown that the electron-hole attraction is largely responsible for the peculiar line shape of the surface reflectance anisotropy.

DOI: 10.1103/PhysRevLett.88.016402

PACS numbers: 71.15.Qe, 73.20.At, 78.66.Db

The correct understanding and modeling of surface optical properties has been a long standing issue of scientific interest. Techniques such as reflectance anisotropy/difference spectroscopy (RAS/RDS) have evolved from experimental methods to characterize static surfaces to very powerful *in situ* diagnostic probes which allow for the monitoring and controlling of the surface growth in real time and in challenging environments such as in high pressures or under liquids [1]. However, somewhat in contrast to their frequent use, the present understanding of the physical origin of the observed optical phenomena is still rather limited.

Aspnes and Studna [2] discriminated between two components of surface optical spectra: “intrinsic” contributions arising from optical transitions within the bulk and “extrinsic” contributions directly related to the surface chemistry. The latter can often be traced to specific surface electronic states and serve as fingerprints for surface structural motifs [3,4]. The origin of the intrinsic features, however, is harder to explain. It has been discussed for a long time that these features are likely to be related to many-particle effects [5] and/or surface local fields (LF) [6,7], i.e., the influence of the surface-modified microscopic fluctuations of the electric field on the macroscopic dielectric response. However, no definite assignment has been possible yet.

This is largely due to the numerical expense required for converged calculations of surface optical properties. In particular, the intrinsic features of the surface spectra are caused by electronic transitions involving a very large number of surface-modified bulk wave functions [3]. Therefore even calculations assuming a single-particle picture for electronic excitations and neglecting self-energy effects are quite involved for surfaces. The inclusion of many-particle effects such as electron-electron and electron-hole interactions dramatically increases the computational cost. Although exact expressions for the excitonic and LF contributions to the surface optical response based on the Bethe-Salpeter equation (BSE) have been derived decades ago, their application has been limited to very few tight-binding (TB) studies [8]. Because of the complexity of the problem, another, more frequently used approach approximates LF effects by modeling the

crystal surface by a lattice of polarizable entities, which obey a Clausius-Mossotti-like relation [6,7,9]. Obviously, such models as well as TB calculations necessarily depend on external input parameters and cannot account accurately for the surface induced changes of the electronic structure. Very recently, it has become possible to solve the BSE from *first principles* for bulk semiconductors [10,11] and strongly localized surface states [12]. However, the large numerical effort has restricted such calculations to the interaction of relatively few electron-hole pairs. As yet they have not been applied to the surface optical response in a wide spectral range.

Here we use an alternative approach to solve the BSE that allows for the study of large systems such as surfaces. It is shown that many-particle effects on the energies and oscillator strengths of electronic excitations in bulklike layers are largely responsible for the appearance of the intrinsic features in surface optical spectra. In particular the electron-hole interaction may influence the magnitude and line shape of spectral features.

We use the hydrogen-passivated Si(110) surface as a model system. It is one of the first systems studied by RAS [2] and its optical features are mainly intrinsic in character. The passivation of the Si dangling bonds results in there being no surface states in the energy region probed by RAS. The surface spectrum is rather insensitive to the structural and chemical details of the passivation [2,13,14] and has a very characteristic line shape with maxima close to the  $E_1$  and  $E_2$  critical point energies of bulk silicon. Because the RAS spectrum can be easily reproduced, it has become a calibration standard for RAS apparatus and a textbook example for surface optical properties [15].

The physical mechanism leading to the observed line shape, however, is not understood. In their original study [2] Aspnes and Studna argued that the measurements are indicative for the appearance of surface local fields and/or many-body screening. The strong influence of local fields seems to be supported by model calculations [6,9]. TB studies that neglected LF effects [16] failed to describe the experiment, as did a TB work that included an approximation for LF effects [7]. In the latter study it was concluded that surface defects are responsible for the

experimentally observed peaks. While real surfaces do contain defects, their RAS contributions should be small in that specific case, since the measured spectrum is nearly independent from the surface preparation procedures [2,13,14]. Indeed, a recent *ab initio* calculation [17] that approximated self-energy corrections using a scissors operator, but neglected LF and excitonic effects, showed that a hydrogen-terminated Si(110) surface gives rise to optical anisotropies at the bulk critical points without the assumption of surface defects. This work, however, could not account for the peculiar line shape observed experimentally.

We go beyond these previous studies and present a consistent and detailed analysis of how electronic self-energy, LF, and excitonic effects manifest themselves in the optical spectrum of Si(110):H. Thereby we proceed in three steps: (i) local density-functional (DFT-LDA) calculations yield the structurally relaxed ground state configuration of the surface, including the Kohn-Sham eigenvalues and eigenfunctions that enter the single- and two-particle Green's functions; (ii) the electronic quasiparticle spectrum is obtained within the *GW* approximation [18] to the exchange correlation self-energy; and (iii) the BSE is solved for coupled electron-hole excitations [10–12]. Thereby the screened electron-hole attraction and the unscreened electron-hole exchange are taken into account [19]. Inclusion of the latter allows for a parameter-free calculation of the LF effects. For surfaces, LF effects can be expected from both the microscopic fluctuations of the electric field within the bulk, and from the truncation of the bulk itself. The resulting macroscopic polarizabilities are finally used to compute the reflectance anisotropy for normally incident light polarized parallel to the  $[1\bar{1}0]$  and  $[001]$  directions [20].

The surface is modeled by periodic supercells containing 12 atomic Si layers. Silicon dangling bonds at the bottom and top layer are saturated with hydrogen. A vacuum region equivalent to 8 atomic layers in thickness separates the material slabs in  $[110]$  direction. Apart from the atoms of the innermost two layers which were kept in their ideal bulk positions, all atomic coordinates are fully relaxed. Four  $\mathbf{k}$  points in the irreducible part of the surface Brillouin zone are used for the self-consistent calculation of the ground-state charge density. For the calculation of the surface optical properties we use 140 uniformly distributed  $\mathbf{k}$  points.

In detail, we start from *first-principles* pseudopotential calculations, using a massively parallel real-space finite-difference implementation of the DFT-LDA [21]. A multigrid technique is used for convergence acceleration. In the second step we include electronic self-energy effects. This requires the replacement of the LDA exchange and correlation potential by the nonlocal and energy-dependent self-energy operator  $\Sigma(\mathbf{r}, \mathbf{r}'; E)$ . We calculate  $\Sigma$  in the *GW* approximation [18], where it is expressed as a convolution of the single-particle propagator  $G$  and the dynamically screened Coulomb interaction  $W$ . Since the calculation of surface optical spectra involves a very large number of electronic states, we introduce further approximations and use a model dielectric function [22] to calculate  $W$ . This speeds up the calculations substantially and results in bulk and surface quasiparticle energies which are within about 0.1 eV of the complete calculations [3,23]. The electron-hole interaction is taken into account in the third step. The inhomogeneous BSE for the polarization function determining the macroscopic optical polarization is transformed into an effective two-particle eigenvalue problem for the coupled electron-hole excitations. The two-particle Hamiltonian

$$H_{v\mathbf{c}\mathbf{k}, v'\mathbf{c}'\mathbf{k}'} = (\epsilon_{c\mathbf{k}} - \epsilon_{v\mathbf{k}})\delta_{vv'}\delta_{cc'}\delta_{\mathbf{k},\mathbf{k}'} + 2 \iint d\mathbf{x} d\mathbf{x}' \psi_{c\mathbf{k}}^*(\mathbf{x})\psi_{v\mathbf{k}}(\mathbf{x})\bar{v}(\mathbf{x} - \mathbf{x}')\psi_{c'\mathbf{k}'}(\mathbf{x}')\psi_{v'\mathbf{k}'}^*(\mathbf{x}') - \iint d\mathbf{x} d\mathbf{x}' \psi_{c\mathbf{k}}^*(\mathbf{x})\psi_{c'\mathbf{k}'}(\mathbf{x})W(\mathbf{x}, \mathbf{x}')\psi_{v\mathbf{k}}(\mathbf{x}')\psi_{v'\mathbf{k}'}^*(\mathbf{x}') \quad (1)$$

describes the interaction of pairs of electrons in conduction states  $|c\mathbf{k}\rangle$  and holes in valence states  $|v\mathbf{k}\rangle$  [19]. It consists of three parts. The diagonal first part is given by the quasiparticle energies obtained in the *GW* approximation. The second, exchange-interaction term, where the short-range part of the bare Coulomb potential  $\bar{v}$  enters, reflects the influence of local fields. The third part, finally, which we calculate using the same approximations for  $W$  as in the self-energy, describes the screened electron-hole attraction.

The eigenvalues and eigenvectors of the two-particle Hamiltonian (1) determined by matrix-diagonalization techniques can be used to calculate the macroscopic dielectric function. While this works perfectly for a relatively small number of electron-hole pair states [10,12], direct diagonalization techniques are prohibitively expensive for systems described by many electronic states

such as those studied here. The dimension of the exciton Hamiltonian for the 12 layer slab used to model the Si(110):H surface is  $N = N_v \times N_c \times N_{\mathbf{k}} = 350\,000$ . In order to avoid the diagonalization bottleneck we followed an idea by Glutsch *et al.* [24]: If the energy dependence of the macroscopic polarizability on the eigenvalues of the exciton Hamiltonian is Fourier transformed, the polarizability can be obtained from the solution of an initial-value problem for a vector  $|\mu(t)\rangle$ , the time evolution of which is driven by the pair Hamiltonian (1)

$$i\hbar|\dot{\mu}(t)\rangle = H|\mu(t)\rangle. \quad (2)$$

The initial values of the vector elements are given by

$$\mu_{cv\mathbf{k}}^i(0) = \frac{\langle c\mathbf{k}|v_i|v\mathbf{k}\rangle}{\epsilon_{c\mathbf{k}}^{\text{LDA}} - \epsilon_{v\mathbf{k}}^{\text{LDA}}}, \quad (3)$$

where  $v_i$  is the  $i$  ( $= x, y, z$ ) component of the velocity operator. The macroscopic dielectric function with the broadening parameter  $\gamma$  is then obtained by the Fourier transform of  $e^{-\gamma t} \langle \mu(0) | \mu(t) \rangle$ . We solve the initial-value problem by the central difference (“leap-frog”) method with the matrix-vector multiplications distributed on many processors. The upper limit of the Fourier integral can be truncated, due to the exponential  $e^{-\gamma t}$ . The number of time steps, i.e., matrix-vector multiplications, is nearly independent of the dimension of the system. The operation count for this method (details will be published elsewhere) scales thus with  $\mathcal{O}(N^2)$  as compared to the  $\mathcal{O}(N^3)$  for the matrix diagonalization. It is therefore particularly suitable for systems with many electron-hole pair states  $N$ .

Figure 1 contains the calculated RAS spectra for the Si(110):H surface represented by a 12-layer slab. The DFT-LDA spectrum shows two strong positive RAS features near the  $E_1$  and  $E_2$  bulk critical point energies. However, the features are far too broad. This is partially due to the coarse  $\mathbf{k}$ -point sampling and a slab which is too thin to allow for a complete description of the surface-perturbed bulk wave functions responsible for the observed optical anisotropies. Denser  $\mathbf{k}$ -point meshes and thicker slabs lead to a much better description of the optical anisotropy at the  $E_2$  energy (see Fig. 3 in Ref. [17]). They do not improve the poor representation of the line shape and strength of the anisotropy at the  $E_1$  energy, however. Inclusion of quasi-particle effects in  $GW$  approximation leads to a blueshift of the spectrum by about 0.6–0.7 eV and changes the line shape. In particular, the anisotropy at the  $E_1$  energy is en-

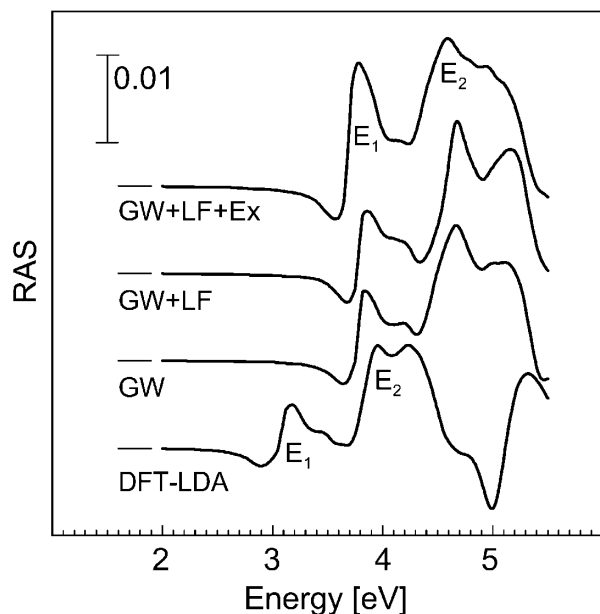


FIG. 1. RAS spectra  $[\text{Re}\{(r_{[1\bar{1}0]} - r_{[001]})/\langle r \rangle\}]$  calculated for Si(110):H described by a 12-layer slab. The notation refers to calculations within DFT-LDA, in  $GW$  approximation, in  $GW$  approximation with the effects of local fields included, and in  $GW$  approximation with the effects of local fields and the electron-hole attraction included.

hanced compared to the DFT-LDA spectrum. The  $E_1$  peak height relative to the  $E_2$  anisotropy is still much smaller than measured, however. LF effects lead to surprisingly small changes of the spectrum. We find a reduction of the calculated slab polarizabilities upon inclusion of LF effects comparable to the one calculated for bulk Si. The reduction acts both on the  $\alpha_{[001]}$  and the  $\alpha_{[1\bar{1}0]}$  tensor components. It is therefore largely canceled in the optical anisotropy. Rather than increasing the ratio of the  $E_1/E_2$  peak heights, LF effects even lead to a small decrease. A drastic enhancement of the optical anisotropy at the  $E_1$  energy and a redshift of the entire spectrum by about 0.1–0.2 eV result, however, from the inclusion of the attractive electron-hole interaction. This is shown by the uppermost spectrum in Fig. 1. Also the characteristic negative anisotropy below the  $E_1$  energy is enhanced by excitonic effects.

Figure 2 shows the calculated slab polarizability. The  $[1\bar{1}0]$  component, i.e., the component probed by light with a polarization direction parallel to the Si-Si zigzag chains shows a strong peak close to the  $E_1$  energy. On the other hand, the  $\alpha_{[001]}$  component has only a weak shoulder at the  $E_1$  energy. This difference is responsible for the strong optical anisotropies measured for passivated Si(110) surfaces.

The stepwise inclusion of many-particle effects in the calculation leads to a considerable and systematic improvement of the agreement with the experiment. However, even the uppermost curve in Fig. 1 still deviates from the measured data. On the one hand, this concerns the line shape around the  $E_2$  peak. This is mainly due to the insufficient thickness of our slab. That can be seen from DFT-LDA calculations [17] which are computationally far less expensive and can thus be extended to full numerical convergence. For the comparison with the experimental data [13] shown in Fig. 3 we have therefore extrapolated

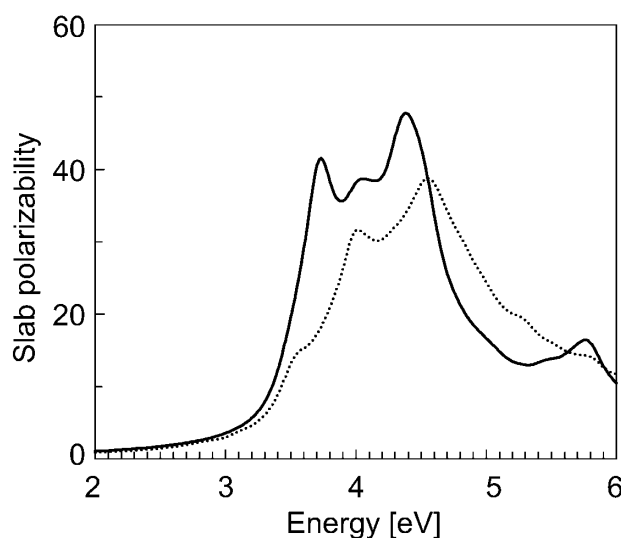


FIG. 2. Imaginary parts of the  $\alpha_{[1\bar{1}0]}$  (solid line) and  $\alpha_{[001]}$  components of the slab polarizability calculated for Si(110):H in  $GW$  approximation with the effects of local fields and the electron-hole attraction included.

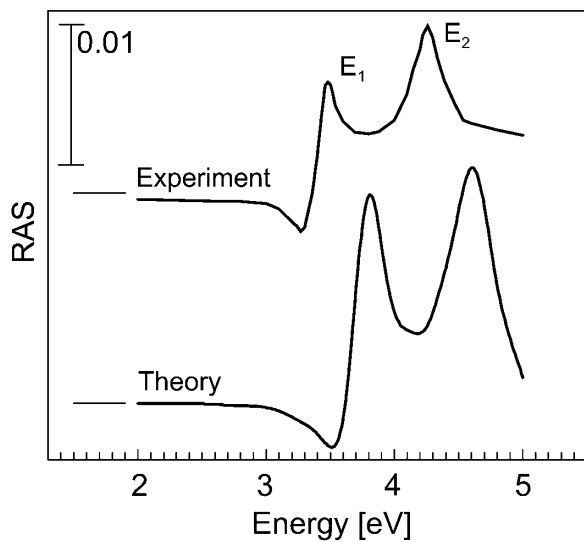


FIG. 3. Measured data for Si(110):H from Ref. [13] are compared with the extrapolation of the  $GW + LF + Ex$  curve from Fig. 1 to calculations for a 24-layer slab (see text).

our calculated spectrum to a thicker slab by adding the difference between the “ $GW + LF + Ex$ ” and “ $GW$ ” curves from Fig. 1 to the RAS spectrum of Si(110):H calculated in  $GW$  approximation for a 24-layer slab. This simple procedure leads to a rather good description of the measured line shape. However, there remains still another discrepancy between calculation and experiment: The calculated peak positions occur at energies that are about 0.3 eV too high. Our calculations were performed at the theoretical equilibrium lattice constant of 5.378 Å. That leads to an increase of the energy splitting between occupied and empty states by about 0.1 eV compared to calculations at the experimental lattice constant. Temperature effects in the measured spectra which are neglected in our calculations result in a redshift of the optical spectra by a similar amount [25]. The remaining difference to the experiment is related to numerical insufficiencies as the relatively small number of  $\mathbf{k}$  points and our approximations in calculating the screened Coulomb potential  $W$ . The latter tend to lead to slightly overestimated excitation energies [22].

In summary, we have demonstrated that by using a time-evolution rather than a matrix-diagonalization technique for the solution of the Bethe-Salpeter equation, it is now possible to include excitonic and local-field effects in the calculation of optical properties of complex systems consisting of many atoms. We calculated the optical anisotropy of the prototypical Si(110):H surface, the origin of which has been the subject of a long-standing controversy. It is shown that excitonic effects via strong modifications of the optical response of surface-modified bulk wave functions determine largely the line shape of the optical features. Local-field effects are found to play a much smaller role than previously thought. We expect the method presented here to be extremely useful for the accurate calcu-

lation of optical properties for many more systems characterized by a large number of electron-hole pairs.

We thank S. Glutsch, L. Reining, and V. Olevano for very helpful discussions. Grants of computer time from the Leibniz-Rechenzentrum München, the John von Neumann-Institut Jülich, and the Höchstleistungsrechenzentrum Stuttgart are gratefully acknowledged. The work was supported by the EU Research Training Network NANOPHASE (HPRN-CT-2000-00167).

- [1] D. E. Aspnes, *Solid State Commun.* **101**, 85 (1997).
- [2] D. E. Aspnes and A. A. Studna, *Phys. Rev. Lett.* **54**, 1956 (1985).
- [3] W. G. Schmidt *et al.*, *Phys. Rev. B* **61**, R16 335 (2000); W. G. Schmidt, F. Bechstedt, and J. Bernholc, *J. Vac. Sci. Technol. B* **18**, 2215 (2000).
- [4] W. Lu, W. G. Schmidt, E. L. Briggs, and J. Bernholc, *Phys. Rev. Lett.* **85**, 4381 (2000).
- [5] L. Mantese, K. A. Bell, D. E. Aspnes, and U. Rossow, *Phys. Lett. A* **253**, 93 (1999).
- [6] W. L. Mochán and R. G. Barrera, *Phys. Rev. Lett.* **55**, 1192 (1985).
- [7] B. S. Mendoza, R. Del Sole, and A. I. Shkrebtii, *Phys. Rev. B* **57**, R12 709 (1998).
- [8] C. H. Wu and W. Hanke, *Solid State Commun.* **23**, 829 (1977); R. Del Sole and E. Fiorino, *Phys. Rev. B* **29**, 4631 (1984); R. Del Sole and A. Selloni, *Phys. Rev. B* **30**, 883 (1984).
- [9] B. S. Mendoza and W. L. Mochán, *Phys. Rev. B* **55**, 2489 (1997).
- [10] S. Albrecht, L. Reining, R. Del Sole, and G. Onida, *Phys. Rev. Lett.* **80**, 4510 (1998).
- [11] L. X. Benedict, E. L. Shirley, and R. B. Bohn, *Phys. Rev. Lett.* **80**, 4514 (1998).
- [12] M. Rohlfing and S. G. Louie, *Phys. Rev. Lett.* **83**, 856 (1999).
- [13] T. Yasuda *et al.*, *J. Vac. Sci. Technol. A* **12**, 1152 (1994).
- [14] K. Hingerl *et al.*, *Appl. Surf. Sci.* **175**, 769 (2001).
- [15] P. Y. Yu and M. Cardona, *Fundamentals of Semiconductors* (Springer-Verlag, Berlin, 1999).
- [16] A. Selloni, P. Marsella, and R. Del Sole, *Phys. Rev. B* **33**, 8885 (1986).
- [17] W. G. Schmidt and J. Bernholc, *Phys. Rev. B* **61**, 7604 (2000).
- [18] M. S. Hybertsen and S. G. Louie, *Phys. Rev. B* **34**, 5390 (1986).
- [19] L. J. Sham and T. M. Rice, *Phys. Rev.* **144**, 708 (1966); W. Hanke and L. J. Sham, *Phys. Rev. B* **12**, 4501 (1975); **21**, 4656 (1980).
- [20] R. Del Sole, *Solid State Commun.* **37**, 537 (1981).
- [21] E. L. Briggs, D. J. Sullivan, and J. Bernholc, *Phys. Rev. B* **54**, 14 362 (1996).
- [22] F. Bechstedt, R. Del Sole, G. Cappellini, and L. Reining, *Solid State Commun.* **84**, 765 (1992).
- [23] J. E. Northrup, *Phys. Rev. B* **47**, 10 032 (1993).
- [24] S. Glutsch, D. S. Chemla, and F. Bechstedt, *Phys. Rev. B* **54**, 11 592 (1996).
- [25] P. Lautenschlager, M. Garriga, L. Viña, and M. Cardona, *Phys. Rev. B* **36**, 4821 (1987).